Journal of Reinforced Plastics and Composites
http://jrp.sagepub.com/

Micro-structural, thermal, and mechanical properties of injection-molded glass fiber/nanoclay/polypropylene composites

Normasmira Abd. Rahman, Aziz Hassan, Rosiyah Yahya, R.A. Lafia-Araga and Peter R. Hornsby

Journal of Reinforced Plastics and Composites 2012 31: 269 originally published online 13 February 2012
DOI: 10.1177/0731684411435727

The online version of this article can be found at:
http://jrp.sagepub.com/content/31/4/269

Published by:
SAGE
http://www.sagepublications.com

Additional services and information for *Journal of Reinforced Plastics and Composites* can be found at:

Email Alerts: http://jrp.sagepub.com/cgi/alerts

Subscriptions: http://jrp.sagepub.com/subscriptions

Reprints: http://www.sagepub.com/journalsReprints.nav

Permissions: http://www.sagepub.com/journalsPermissions.nav

Citations: http://jrp.sagepub.com/content/31/4/269.refs.html

>> Version of Record - Feb 21, 2012

OnlineFirst Version of Record - Feb 13, 2012

What is This?

Downloaded from jrp.sagepub.com at HINARI on March 4, 2012

Article

JOURNAL OF REINFORCED PLASTICS & COMPOSITES

Journal of Reinforced Plastics and Composites
31(4) 269–281
© The Author(s) 2012
Reprints and permissions:
sagepub.co.uk/journalsPermissions.nav
DOI: 10.1177/0731684411435727
jrp.sagepub.com

SAGE

Micro-structural, thermal, and mechanical properties of injection-molded glass fiber/nanoclay/polypropylene composites

Normasmira Abd. Rahman[1], Aziz Hassan[1], Rosiyah Yahya[1], R.A. Lafia-Araga[1] and Peter R. Hornsby[2]

Abstract

Hybrid composites of PP/NC/GF were prepared by extrusion and injection molding. Molded specimens were analyzed by XRD, SEM, and TEM, together with characterization of thermal and mechanical properties. XRD results revealed that the interaction between NC particles and the PP matrix results in intercalation of the polymer chains, which increases the clay interlayer distance. TEM results revealed NC particle intercalation. TGA results showed that the incorporation of clay into the GF composite improves the thermal stability of the material. The initial thermal decomposition temperatures also shifted to higher values. Incorporation of GF into PP lowers the tensile strength of the binary composite, indicating poor fiber–matrix interfacial adhesion; however, introducing NC increased the strength of the ternary composites. Tensile modulus was enhanced with the incorporation of GF and further increased with an introduction of NC. Flexural strength and flexural modulus are both enhanced with an increase in fiber loading. The addition of clay nanoparticles further improved these properties.

Keywords

extrusion, injection molding, mechanical properties, thermal properties, glass fiber/nanoclay/polypropylene composites

Introduction

Polypropylene (PP) is one of the most industrially successful thermoplastic polymers, characterized by its excellent cost-to-performance ratio. The commercial significance of PP has resulted in an ever increasing drive to enhance its properties further, particularly through reinforcement with various particulates, fibers, and layered inorganic fillers.[1–3] The effectiveness of inorganic fillers in improving the physical and mechanical properties of PP strongly depends on the filler aspect ratio, size, shape, surface characteristics, interfacial adhesion, and degree of filler dispersion.[4] It has repeatedly been shown that an inorganic filler such as glass fiber (GF) increases the tensile modulus of such composites, yet causes the decrease of the strength and toughness. It could be due to the stress concentration, poor fiber–matrix adhesion and confinement of the matrix molecular mobility around the rigid filler phase.

A relatively new development in the field of polymer composites is the introduction of clay nanoparticles, in which small quantities of high-modulus nanoclay (NC) particles have been shown to give significant improvements in mechanical, barrier, and thermal properties.[5,6] Although numerous researchers have investigated individually PP/GF composites and PP/NC composite systems, only a few investigations have been reported on PP/GF/NC composites. Mohan and Kanny,[7] in their work, combined the PP nanocomposite matrix with chopped GF. A small amount (5% fiber weight fraction (W_f)) of nanoscale dispersed layered silicate was shown to enhance the degree of crystallinity as well as tensile properties. Using nano-reinforcements in a GF-reinforced vinyl ester matrix, Chandradass

[1]Department of Chemistry, University of Malaya, 50603 Kuala Lumpur, Malaysia.
[2]School of Mechanical and Aerospace Engineering, Queen's University Belfast, Belfast BT9 5AH, United Kingdom.

Corresponding author:
Aziz Hassan, Department of Chemistry, University of Malaya, 50603 Kuala Lumpur, Malaysia
Email: ahassan@um.edu.my

Downloaded from jrp.sagepub.com at HINARI on March 4, 2012

et al.[8] observed that the addition of 3% W_f of NC gave the highest increment in tensile, flexural, and impact properties.

In this study, PP/clay nanocomposite systems were prepared for use as a matrix material for GF composites. An experimental study was carried out to exploit the functional advantages and potentially synergistic effect on GF and NC in order to enhance the overall properties of PP. As a comparison, the properties of PP/GF composite and PP/NC nanocomposite were also evaluated under identical test conditions. The structures of PP/NC and PP/GF/NC were investigated by X-ray diffraction (XRD), scanning electron (SEM) and transmission electron (TEM) microscopies. Thermal and mechanical properties of the composites were also investigated by thermogravimetric analysis (TGA), tensile, and flexural tests, respectively.

Experimental procedures

Materials

PP (Propelinas H022) was supplied by Petronas, Malaysia. The neat PP was in the form of pellets with a melt flow index of 11 g·10 min^{-1} and a density of 910 kg·m^{-3}. Chopped E-GF, surface-treated with silane and having a density 2550 kg·m^{-3}, diameter 14 μm and length 6 mm, obtained from KCC Corporation, Korea, was used as the principal reinforcement. The NC (type PGV) is a natural montmorillonite clay with a density of 776 kg·m^{-3} and a particle size of about 16 μm and manufactured by Nanocor, USA.

Specimen preparation

PP/GF and PP/NC composites were prepared with different ratios of PP/chopped GF and PP/clay powder, respectively, as presented in Table 1. Compositions were physically pre-mixed, mixed, and then compounded using a Brabender (KETSE 20/40) twin screw extruder. The temperature profile was set to 185–190°C. For the PP/GF composites, the screw speed was set to 100 rpm, whereas for the PP/NC composites 800 rpm. The materials extruded from both formulations were pelletized into length of about 6 mm. In order to produce PP/GF/NC composites, the different ratios of the PP/NC and chopped GF were physically mixed and re-compounded in a twin screw extruder using the same temperature profile and screw speed 100 rpm. Dumbbell-shaped tensile test specimens,[9] with geometry defined in the ASTM standard D638, were then injection molded using a Boy® 55M, a 55 tonne injection molding machine. The processing temperature was set between 175°C and 185°C and the mold temperature at 25°C. The list and abbreviation of specimens prepared are given in Table 1. Specimens were designated according to their composition; for example, (PP85/G15)/NC3 was referred as specimen with 85 wt% of PP, 15 wt% of GF, and 3 phr of NC.

Microstructural characterization

Neat clay, PP/NC, and PP/GF/NC were analyzed by XRD using Philips binary diffractometer with Cu-K_α radiation. Powder clay and nanocomposite tensile specimens were scanned over the interval of $2\theta = 2° - 30°$ at 40 kV and 30 mA. Using XRD, intercalation behavior of clay particles (in the composites) with different concentration was analyzed.

The fracture surface of the various nanocomposites was examined using a Field Emission Auger Microprobe model JAMP-9500F under SEM mode to investigate the effects of clay loading on the adhesion at

Table 1. Designation and compositions of composite specimens

Sample	Matrix weight fraction, W_m (%)	Fiber weight fraction, W_f (%)	Fiber volume fraction, V_f (%)	Clay content (phr)
NC (clay)	–	–	–	–
PP	100	–	–	–
PP85/G15	85	15	6	–
PP70/G30	70	30	14	–
PP100/NC3	100	–	–	3
PP100/NC6	100	–	–	6
PP100/NC9	100	–	–	9
(PP85/G15)/NC3	85	15	6	3
(PP85/G15)/NC6	85	15	6	6
(PP85/G15)/NC9	85	15	6	9
(PP70/G30)/NC6	70	30	14	6

Downloaded from jrp.sagepub.com at HINARI on March 4, 2012

the interface between GF and the PP matrix and the extent of clay dispersion. SEM micrographs were taken at an acceleration voltage of 10 keV at various magnifications. The fractured surface of tensile specimens was sputter-coated with a thin layer of gold in order to improve the sample conductivity and to avoid electrical charging during examination.

The microstructure of the PP/NC and PP/GF/NC were analyzed with a Hitachi H-600 (Japan) TEM. The samples were ultra-microtomed with a diamond knife on a Leica Ultracut UCT (UK) microtome at room temperature to give sections with a nominal thickness of 200 nm. Sections were transferred to 400-mesh Cu grids. Bright-field TEM images of the composites were obtained at 300 kV under low-dose conditions.

Thermogravimetric analysis

TGA analysis was done using a TGA 6 thermogravimetric analyzer (Perkin Elmer) to study the thermal decomposition behavior of the composites. Tests were done under nitrogen environment at a scan rate of

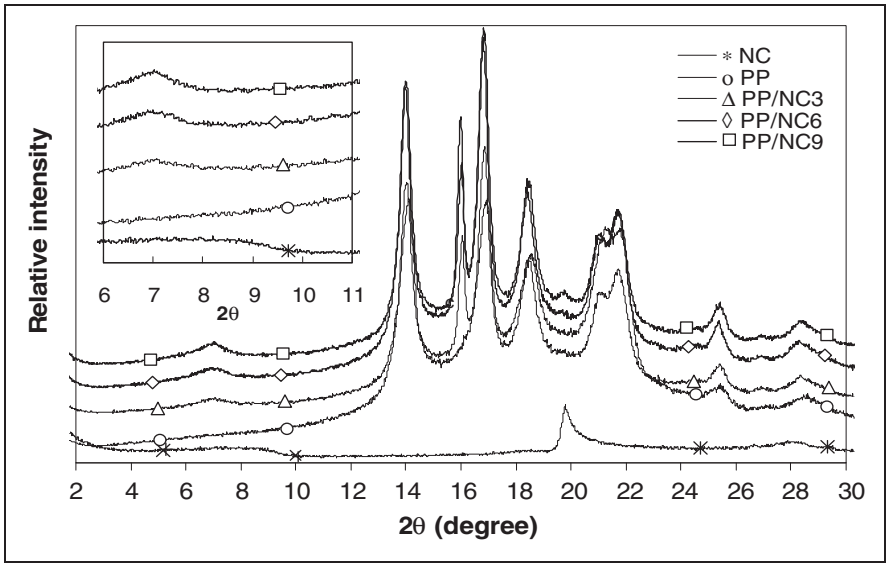

Figure 1. The XRD patterns of PP/NC nanocomposites.

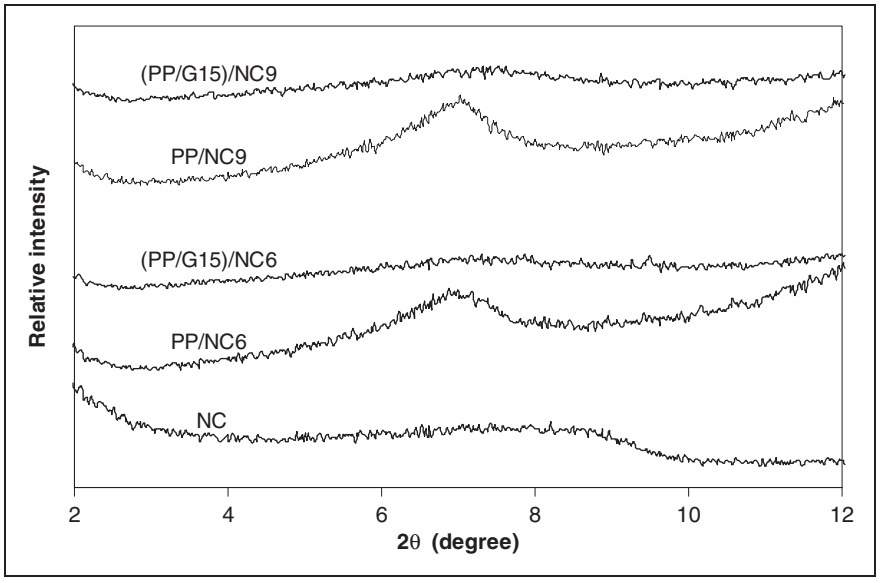

Figure 2. The XRD patterns of PP/NC and PP/GF/NC hybrid composites.

Downloaded from jrp.sagepub.com at HINARI on March 4, 2012

$10^{\circ}C \cdot min^{-1}$ over a programmed temperature range 50–850°C. A test sample of 5–10 mg was used for each run.

Mechanical property characterization

Tensile tests were carried out using a universal testing machine, Instron 5569 (50 kN load-cell) at a constant cross-head speed of $5\,mm \cdot min^{-1}$ at 25°C. The tensile properties were determined[9] according to the ASTM D638. The composite modulus was recorded at 0.5% strain.

Flexural tests[10] were carried out using the same machine and following the ASTM D790 method. The distance between the support spans was 50 cm. All the specimens were tested at a constant cross-head speed of $1.28\,mm \cdot min^{-1}$.

Results and discussion

Microstructure

XRD showed that intercalation of the polymer between the layers of the clay had occurred, resulting in an increased clay interlayer distance. It has been shown by several researchers[11,12] that this method can be used to observe how layered nanoparticles are distributed in a polymer and can be employed to characterize their degree of dispersion. Bragg's equation is typically employed to measure the interlayer distance using the diffraction peak and its position in the XRD patterns.[13] It is typically shown as $n\lambda = 2d \sin\theta$, where λ, d, and θ are wavelength (1.54 Å), interlayer spacing, and the diffraction angle, respectively.

In Figures 1 and 2, the data are displayed as the relative intensity of the reflections vs. the scattering angle, 2θ. Table 2 summarizes the XRD data obtained. The characteristic diffraction peak of neat clay is located at around 8.9°, corresponding to a basal interlayer spacing of 1.00 nm according to Bragg's equation. Figure 1 displays the XRD patterns of PP/NC composites by direct melt intercalation with varying clay contents. As shown in the figure, the characteristic peak of clay in the composites was shifted to a lower angle, which indicates that the interlayer d-spacing of clay has been increased.

With dispersion of the clay nanoparticles into PP matrix, the interlayer spacing of the clay in PP/NC composites increased by up to 28%, when compared with the neat clay (Table 2). The interlayer distances of clay are increased from the original 1.00 nm (neat clay) to 1.27, 1.28, and 1.25 nm for PP/NC3, PP/NC6, and PP/NC9, respectively. Although intercalation had occurred, it was evident that some long-range stacking order still remained, as explained by Timmerman et al.[14] Even though clay layers in composites are expanded to a larger extent when compared to neat clay, its characteristic diffraction still exists, which means that some clay layers still retained their original crystal structure and exist as primary particles.[15] The XRD data show that the characteristic diffraction peak of PP/NC composites is almost similar for all systems (3, 6, and 9 phr). Further incorporation of clay into the system only affects the width and intensity of the diffraction peak. However, the diffraction angles remain almost the same. The peak intensity increased by 28% and 44% for 6 and 9 phr composites, respectively, relative to 3 phr composite. This observation suggests that as the concentration of the clay increased (from 3 to 9 phr), more ordered structures were obtained, resulting in a relatively higher fraction of clay agglomeration. As indicated above, the amount of matrix in the composites was constant for all compositions prepared (PP/NC3-9). As the clay content increases, the amount of available matrix for clay intercalation reduces. This results in a decrease in the interlayer d-spacing, as observed from Table 2.

Figure 2 illustrates the XRD diffractograms for NC, PP/NC, and PP/GF/NC composites. The interlayer d-spacing of clay reduces from 1.28 nm (PP/NC6) to 1.25 nm (PP/G15)/NC6 and from 1.25 nm (PP/NC9) to 1.19 nm (PP/G15)/NC9. However, as shown in Figure 2 and Table 2, in addition to reducing the interlayer spacing, introduction of GF in clay nanocomposites broadens the peak as well as decreases its intensity by 62% and 63% for (PP/G15)/NC6 and (PP/G15)/NC9, relative to PP/NC6 and PP/NC9, respectively. This suggests that even though clay still partially keeps the original crystal structure and exists as primary particle, at the same time, it, however, could be partially exfoliated from the stacks of clay layers due to the existence of GF.

As indicated above, PP/NC6 and PP/NC9 composites have been used as matrices for hybridization with 15% W_f GF in order to produce (PP/G15)/NC6 and (PP/G15)/NC9, respectively. From the above

Table 2. XRD data of NC, PP/NC, and PP/GF/NC hybrid composites

Sample	2θ (degrees)	Interlayer spacing (nm)	Peak intensity (counts s^{-1})
NC (clay)	8.86	1.00	127
PP100/NC3	6.97	1.27	251
PP100/NC6	6.88	1.28	321
PP100/NC9	7.04	1.25	362
(PP85/G15)/NC6	7.09	1.25	121
(PP85/G15)/NC9	7.46	1.19	133

Downloaded from jrp.sagepub.com at HINARI on March 4, 2012

discussion, it has been noted that the PP/NC9 has a lower interlayer *d*-spacing (1.25 nm) when compared to PP/NC6 (1.28 nm). Correspondingly, the interlayer spacing of (PP/G15)/NC9 is slightly lower than that of (PP/G15)/NC6. By contrast, Bozkurt et al.[16] suggested that the characteristic peaks from agglomerated clay layers may not be detectable due to the presence of the high fraction of GF in the PP/GF/NC tertiary composite. This would result in the absence or reduction in the characteristic peak intensity.

To analyze the tendency of clay particles to agglomerate, SEM images of the fracture surfaces from tensile specimen of PP/NC and PP/GF/NC composites were obtained, as shown in Figure 3. Figure 3(a) and (b) illustrates the microstructure of the nanocomposites (6 and 9 phr), where the clay is shown as the bright spots in the images. At higher clay concentration (9 phr), a relatively larger clay agglomeration ($\approx$40 μm) is observed, when compared with the 6 phr clay nanocomposite ($\approx$ 35 μm). Agglomeration size was taken from the average of at least five measurements from SEM images. The images agreed with the increase in the peak intensity of the nanocomposite, with higher clay content as obtained from the XRD analysis (Figure 1 and Table 2). Images of the fracture surfaces (Figure 3(c) and (d)) from the PP/GF/NC composites indicate that clay platelets are better dispersed in the composite as compared to those of PP/NC composites (Figure 3(a) and (b)). This implies that the incorporation of GF in the system and the second compounding exercise result in a better dispersion of the particles within the composite. It is obvious that smaller

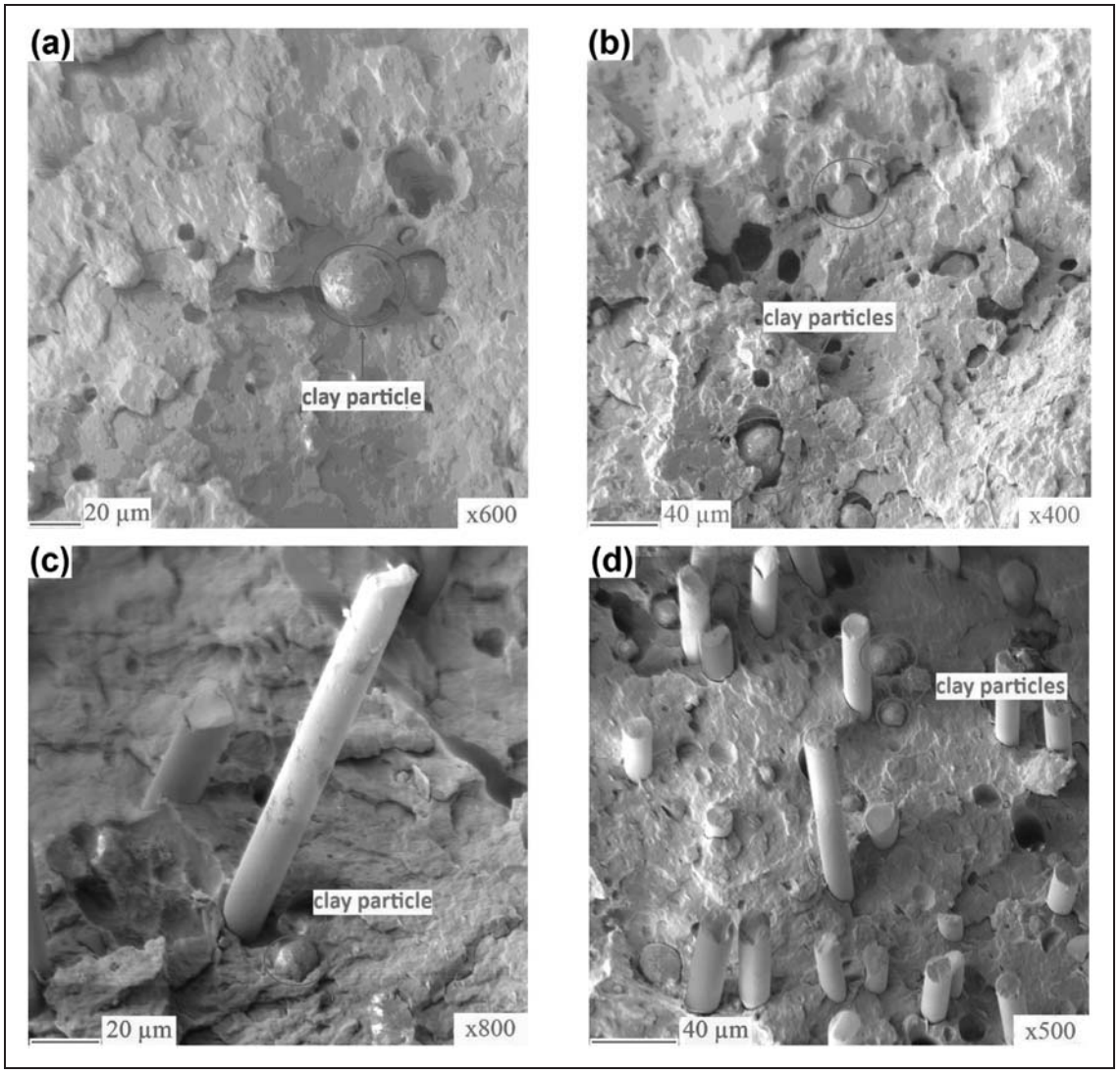

Figure 3. SEM micrographs of tensile fracture surface of (a) PP100/NC6; (b) PP100/NC9; (c) (PP85/G15)/NC6; and (d) (PP85/G15)/NC9 hybrid composites.

Downloaded from jrp.sagepub.com at HINARI on March 4, 2012

agglomerates are formed in the structure of the PP/GF/NC hybrids composites, i.e., ≈14 and 25 μm for PP/GF/NC6 and PP/GF/NC9, respectively, compared with PP/NC composites.

To gain an insight into the NC particle intercalation, characterization using TEM was conducted for PP/NC6 and (PP/G15)/NC6 nanocomposite samples (Figure 4). Both nanocomposites show heterogeneous dispersion, presence of aggregates, as well as resin-rich areas in the matrix without clay. However, there are regions where completely delaminated sheets are dispersed individually, showing dark lines of 1–2 nm, on an average, thickness. It appears that the clay exists as expanded aggregates. Hussain et al.,[17] in their study, suggested that the degree of intercalation or exfoliation depends on type and surface modification of NC, presence of compatibilizing agent, as well as the processing condition.

In Figure 4(a) and (b), the average distance between the clay platelets for PP/NC6 and (PP/G15)/NC6 nanocomposites is 3 and 6 nm, respectively. This observation is interesting as the interlayer spacing for NC in (PP/G15)/NC6 hybrid nanocomposite is expanded compared with PP/NC6 nanocomposites. The presence of the GFs as well as double compounding of the hybrid nanocomposite may have contributed to this expanded interlayer spacing.

Thermogravimetric analysis

The thermal stability of the nanocomposites was studied by the TGA technique. When heating occurs under an inert N_2 gas flow, a non-oxidative degradation occurs, while the use of air or oxygen allows oxidative degradation of the samples.[18] Figure 5 shows the TGA scans in the form of weight change vs. temperature for PP and 15% W_f GF composites containing various amounts of clay nanoparticles (0–9 phr). This provides information about the thermal stability of PP/GF/NC composites, when compared to the corresponding PP/GF composites. Table 3 presents the quantitative values of the onset, derivative peak temperature, and the temperatures at 5%, 10%, and 50% of weight loss, which are referred to as: T_{onset}, DT_P, $T_{5\%}$, $T_{10\%}$, and $T_{50\%}$, respectively. The TGA curves (Figure 5) demonstrate that the incorporation of clay in GF composites improve the thermal stability of the material. Degradation takes place at higher temperature in the presence of clay. The T_{onset} of PP matrix is recorded at 355°C. Incorporation of 15% W_f of GF increases T_{onset} to 422°C. Incorporation of 3, 6, and 9 phr of clay into the composites further increase T_{onset} of (PP/G15)NC to 431°C, 433°C and 436°C, respectively. This behavior could be explained by a diffusion effect when clay is present, which limits the emission of the gaseous degradation products, resulting in an increase in the thermal stability of the material.[19,20]

The initial thermal stability is characterized by the temperatures at 5% and 10% weight change ($T_{5\%}$ and $T_{10\%}$). It can be seen that these initial thermal decomposition temperatures are enhanced by the addition of clay into the GF composite. At 5% weight change, the $T_{5\%}$ increases from 368°C for PP/G15 to 405°C, 420°C and 424°C for composites containing 3, 6, and 9 phr NC, respectively. The same trend is observed at 10% weight change. It is possible that at this initial

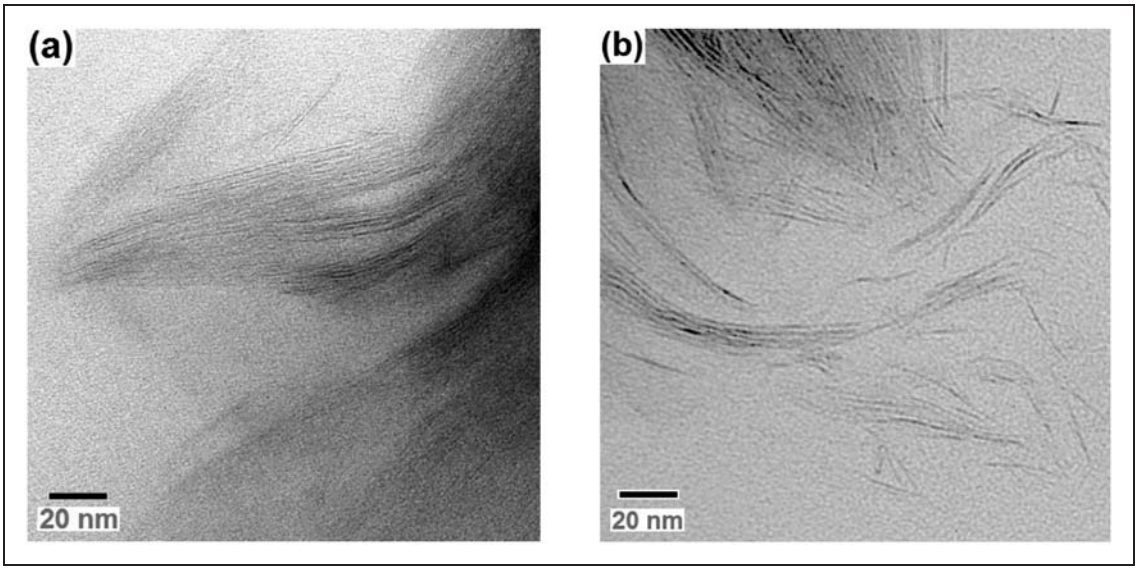

Figure 4. TEM images of (a) PP/NC6 and (b) (PP/G15)/NC6 nanocomposites at high magnification (97,000×).

Downloaded from jrp.sagepub.com at HINARI on March 4, 2012

degradation event, incorporation of NC which invariably enhanced better compatibility between the matrix and the fiber, resulted in a better thermally stable composite (Figure 5). It is believed that the homogenous dispersion of clay platelet acts as a barrier, trapping the volatilizing matrix from escape to atmosphere.

It should be noted from Table 3 and Figure 5 that degradation of PP is completed at about 466°C. It is evident in this figure, that there is a cross-over between degradation curves for PP/G15 and (PP/G15)/NC occurring at 447°C. For comparison, the amount of matrix remaining at this temperature has been calculated for the whole range of specimens, designated as $M_{447°C}$. These values are tabulated in Table 3. Below the cross-over temperature, composites with clay (PP/GF/NC) are more stable, when compared to the one without clay (PP/G15). From the degradation curve for PP, it should be noted that, at temperature of 447°C, only 1% of PP remained. By contrast, at the same temperature, with incorporation of clay into the system, after subtracting the GF and clay content, there is still a large amount of the matrix present, 52% each for (PP/G15)/NC3 and (PP/G15)/NC6 composites and 53% for (PP/G15)/NC9 composite.

By acting as a heat barrier, these high aspect ratio fillers, which not only enhance the overall thermal stability of the system, but also promote char formation, resulting in a high performance carbonaceous silicate layer, insulate the underlying matrix material.[21] Furthermore, at temperatures higher than 447°C, the thermal behavior of GF becomes predominant and an increase in the thermal stability of the GF composite (PP/G15) is observed. This may explain why the values of DT_p and $T_{50\%}$ for PP/G15 are higher than those values for composites with increasing clay loading (Table 3).

Tensile properties

Tensile properties of PP/GF/NC composites with different levels of fiber and clay contents are shown in Figures 6 and 7, which compare with the average tensile strength, modulus, and strain values. For PP/GF composites, the tensile strength decreased as fiber content increased. For example, the tensile strength was reduced from 31 MPa for PP to 28 MPa for PP/G30 composite. This reduction in strength is an indication

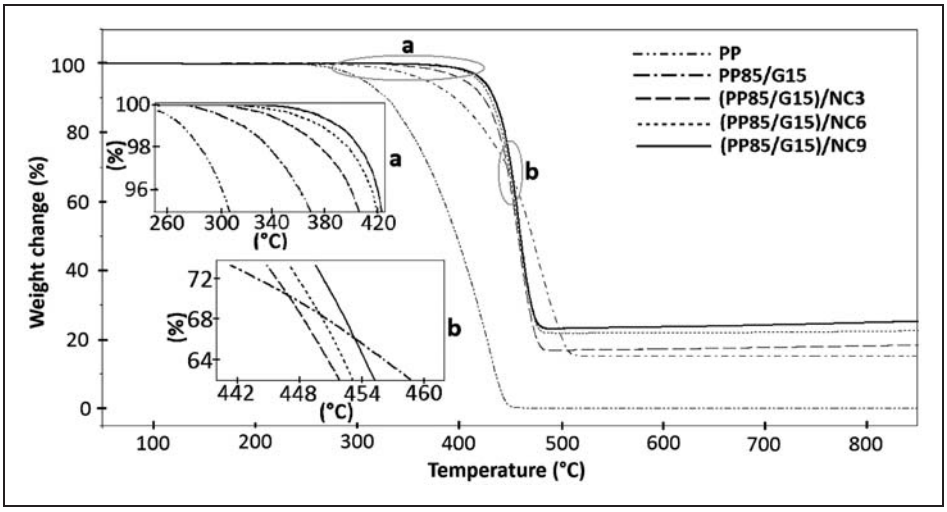

Figure 5. TGA thermograms of PP, PP/GF, and PP/GF/NC hybrid composites.

Table 3. TGA data of PP, PP/GF, and PP/GF/NC hybrid composites

Sample	Decomposition temperature range (°C)	T_{onset} (°C)	$T_{5\%}$ (°C)	$T_{10\%}$ (°C)	$T_{50\%}$ (°C)	DT_P (°C)	$M_{447°C}$ (%)
PP	231–466	355	307	328	397	431	1
PP85/G15	250–525	422	368	392	471	481	55
(PP85/G15)/NC3	321–491	431	405	424	458	458	52
(PP85/G15)/NC6	332–492	433	420	430	459	459	52
(PP85/G15)/NC9	354–494	436	424	435	461	460	53

Downloaded from jrp.sagepub.com at HINARI on March 4, 2012

of poor fiber–matrix adhesion and lack of stress transfer capability of the fiber.[22,23] It is assumed that when there is a poor adhesion at the interface at high deformations, as it happens in these tensile tests, the presence of fillers or fibers in a polymer matrix gives rise to defects at the interface, which are responsible for the strength reduction.[24]

However, the addition of 6 phr clay in 15% W_f, (PP/G15)/NC6 and 30% W_f, (PP/G30)/NC6 resulted in an increase in tensile strength by 10% and 6%, respectively, relative to PP/GF composite at the same fiber loading. It is suggested that the presence of clay increased the interfacial adhesion between GF and PP, hence improving the tensile strength of the PP/GF/NC composite. Since GF and PP are, respectively, inorganic and organic in nature, compatibility between the two is poor. For this reason, GF used in this study was silane treated to improve fiber–matrix

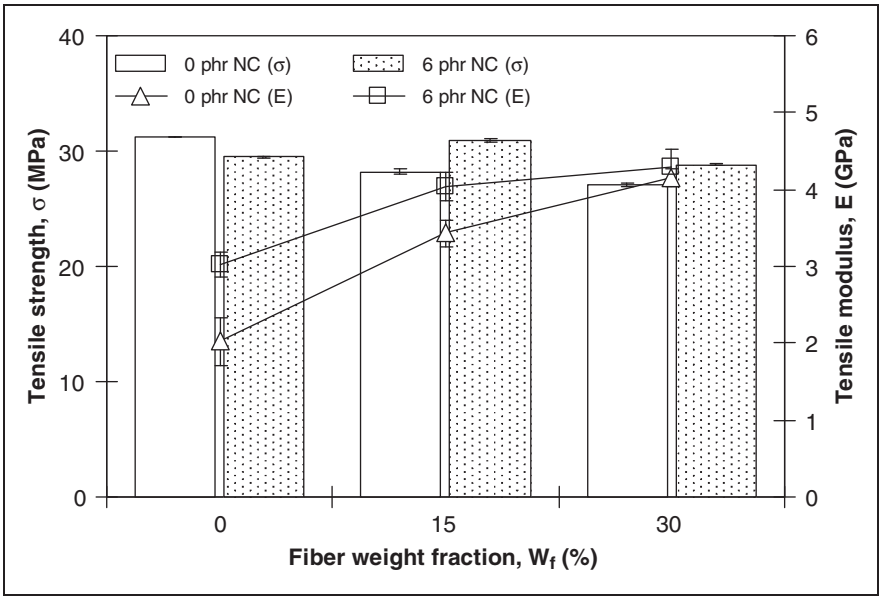

Figure 6. Tensile strength and tensile modulus of PP/GF and PP/GF/NC hybrid composites.

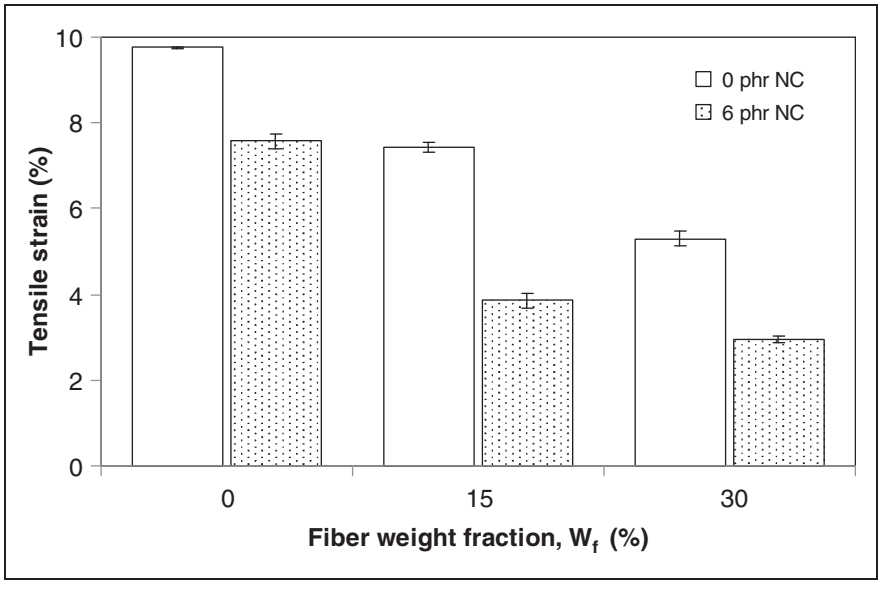

Figure 7. Tensile strain of PP/GF and PP/GF/NC hybrid composites.

Downloaded from jrp.sagepub.com at HINARI on March 4, 2012

interfacial adhesion. It is believed that, apart from improving adhesion between the fiber and matrix, silane treatment also has intensified the synergy between the GF and NC, therefore further enhancing the coupling effect. From microscopic study, it can be seen clearly that the matrix adhere at the GF surface, indicating a good fiber–matrix bonding (Figure 3(c)).

From Figure 6, it can be seen that tensile moduli of composites increased from 70% to 105%, for PP/G15 and PP/G30 composites, respectively, relative to the PP matrix. On the other hand, in the case of (PP/G15)/NC6 and (PP/G30)/NC6, the increase in modulus is more distinct in the order of 100% to 112% upon GF addition, which is in accordance with the trend reported[8] previously. It is revealed from Figure 6 that tensile modulus of PP/NC6 composite increased by 50% (3.02 GPa) when compared to PP matrix (2.02 GPa). It has been reported by other researchers[25] that the improvement of modulus in the hybrid composites (PP/GF/NC) is mainly attributed to the improvement of the matrix modulus from particulate filler dispersion. Thus, it seems that a synergistic effect takes place by incorporating particulate filler into the matrix, leading to higher stiffness than would otherwise be expected, solely on the basis of the change in the matrix modulus. At the same fiber content, the incorporation of NC into the system further enhances the tensile modulus. Modulus of (PP/G15)/NC6 composite increased by about 18%, as clay was added to the system relative to PP/G15. However, at 30% W_f, the effect of NC addition on the tensile modulus is no longer significant. The same behavior has also been reported by Zhao et al.[26] It has been pointed out that when the fibers exceed a certain loading level, the reinforcing efficiency of the fibers will begin to decrease.[27,28] This is because of the wetting problem of the reinforcement phase.

On the other hand, tensile strain (Figure 7) is simultaneously reduced with the incorporation of GF, which is attributed to the fact that reinforcing fibers strongly restrain the deformation of the matrix polymer, as demonstrated in several previous studies.[29–31] The trend remains essentially unchanged as clay nanoparticles are added to the system, except that tensile strain decreases further.

Figure 8 shows the tensile properties of 15% W_f GF composite as a function of NC content. It was observed that the tensile strength and tensile modulus of the composites generally increased with increasing clay content. The tensile strength increased slightly with filler content of 6 phr, beyond which it decreased slightly. An insignificant change (1% reduction) in tensile strength was observed with the addition of 3 phr of clay into PP/GF15 composite. Further addition of 6 phr clay in the matrix, (PP/G15)/NC6 increased the tensile strength by 10%. However, composite, with 9 phr of clay, (PP/G15)/NC6 shows a slight decline in tensile strength. For optimum mechanical properties, there has to be a good dispersion of clay within the composite. From the XRD results, (PP/G15)/NC9 has a lower *d*-spacing, relative to (PP/G15)/NC6 (Figures 2 and 3, and Table 2). Lower interlayer *d*-spacing may mean some agglomeration between the NC in the matrix that causes stress concentration, resulting in

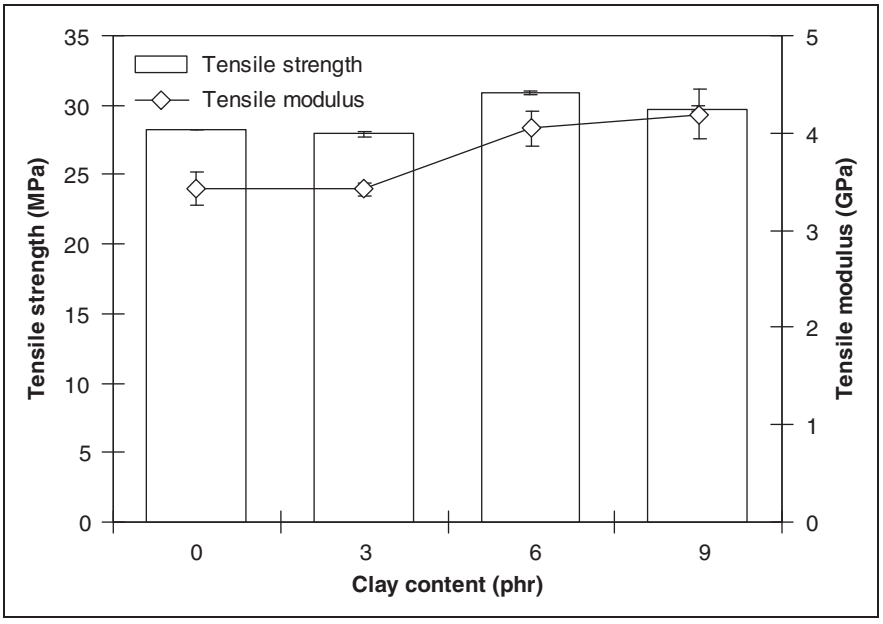

Figure 8. Tensile strength and tensile modulus of 15% W_f GF composite with different clay loadings.

Downloaded from jrp.sagepub.com at HINARI on March 4, 2012

premature failure. Other researchers[32,33] have also reported that the presence of agglomeration in epoxy-GF composites, which obviously caused deterioration in the mechanical properties of the material. On the other hand, higher interlayer *d*-spacing may mean better dispersion of the NC within the matrix and consequently enhancement of properties. This is reflected in the enhancement of tensile strength increment in (PP/G15)/NC6 and a decline of this property in (PP/G15)/NC9 hybrid composites.

It was observed that tensile modulus of hybrid composites increased with increasing clay content (Figure 8). An improvement in tensile modulus of about 22% is observed with an addition of 6 phr clay, relative to PP/G15 composite. The improvement of modulus could be due to the exfoliation of clay nanoparticles in the matrix that restricts the mobility of polymer chains under loading. However, by incorporating 9 phr clay into the composite, only 18% increment in tensile modulus is observed. It has been suggested that at higher clay contents, large agglomerates in the matrix may have occurred, leading to the reduction in tensile modulus.[33] On the other hand, the tensile strain is simultaneously reduced with increase in clay particle content. The tensile strains are reduced from 7% for PP/G15 to 6% for (PP/G15)/NC3 and 4% each for (PP/G15)/NC6 and (PP/G15)/NC9. This can be attributed to the fact that clay particles strongly restrain the deformation of the composites, as demonstrated by Asi[34] in his study.

Flexural properties

Flexural strength and modulus of hybrid nanocomposites are shown in Figures 9 and 10. The PP matrix has a flexural strength of 37 MPa and modulus 1.0 GPa. In Figure 9, the flexural strength and modulus of the GF composites containing 0 and 6 phr clay are shown as functions of the fiber weight fraction. From the results, the effectiveness of clay as reinforcing agent is clearly seen. The PP/GF/NC composites, at all fiber weight fractions, have higher flexural properties (strength and modulus), when compared to the strength of the PP/GF composites. Flexural strength increased by 10%, from 37.3 MPa (PP) to 40.8 MPa (PP/NC6) and 23%, from 42.3 MPa (PP/G15) to 52.1 GPa ((PP/G15)/NC6). The flexural strength of (PP/G15)/NC6 is even higher (52.1 MPa) compared to the strength of composite with 30% W_f fiber (PP70/G30), (46.9 MPa). In the context of this study, even with only a small inclusion (6 phr) of clay in 15% W_f GF composites, materials with a higher flexural strength than the composite with 30% W_f (Figure 9) can be produced. As for the composite with higher fiber weight fraction (PP/G30), only a 6% increment in flexural strength value is observed with the incorporation of 6 phr clay into the system ((PP/G30)/NC6). The same behavior has been observed for the flexural modulus (Figure 9). This could be due to the same reason advanced for the tensile properties that was discussed previously.

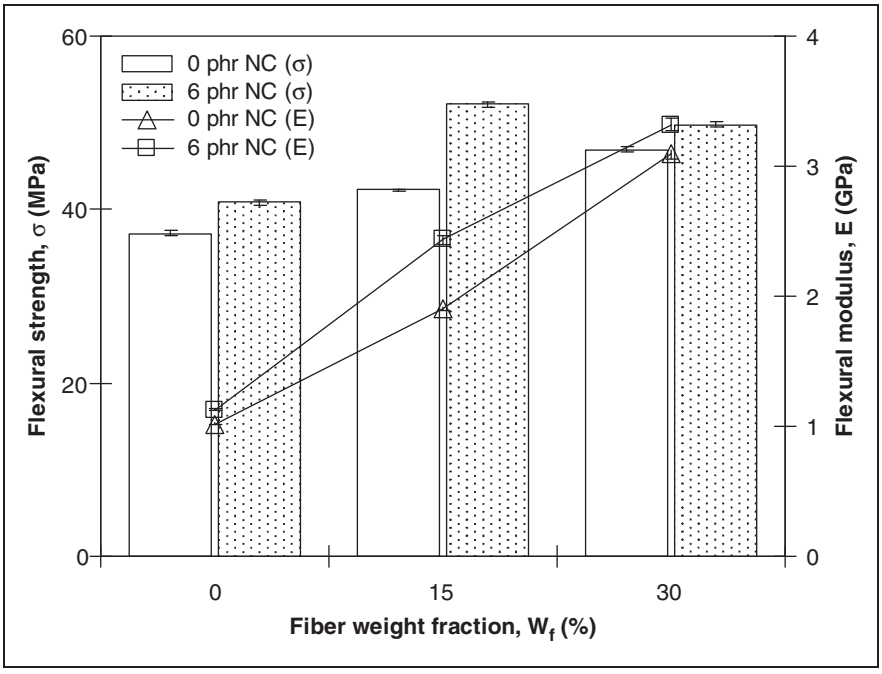

Figure 9. Flexural strength and flexural modulus of PP/GF and PP/GF/NC hybrid composites.

Downloaded from jrp.sagepub.com at HINARI on March 4, 2012

Figure 10 shows the effect of clay loading on the flexural properties (strength and modulus) of 15% W_f composites. From this figure, it can be seen that the flexural strength and flexural modulus of PP/GF composites are monotonically increased, with increase in clay loading, being markedly higher than that of the unfilled PP matrix. Although the flexural failure strength of the composite is a fiber dominant property, the matrix has an influence on the overall properties of the composite. Haque et al.[13] demonstrated that the enhancement in flexural properties of fiber/nanocomposite is achieved due to improved properties of matrix–clay phase composite portion and also unique interfacial fiber–matrix bonding characteristics. Flexural strength of the PP/GF/NC hybrid composites increased by about 14%, 16%, and 40% by the incorporation of 15% W_f GF, 15% W_f GF/3 phr NC, and 15% W_f GF/6 phr NC, relative to the unfilled PP matrix. This is due to the synergistic effects of the GF and NC. Kornmann et al.[35] reported that the strength of the matrix is improved by the presence of the silicate layer. GF and NC appear to provide a good combination of reinforcements to carry the load during the flexural deformation of the composite. However, it is also observed that the optimum flexural strength was achieved at 6 phr clay (52.1 MPa). At 9 phr NC loading, the flexural strength decreases to 51.0 MPa. The distribution of particles in the matrix is an important factor to be considered in this case. The possibility for agglomeration formation is greater at higher clay contents, due to a stress concentrating effect. The same behavior has been reported by other researchers.[8,34,35]

The incorporation of clay yields a significant improvement in the flexural modulus of the PP/GF composites, which is attributed to the stiffness and rigidity of the clay nanoparticles (Figure 10). The flexural modulus increased from 1.01 GPa (PP) to 1.91 GPa (87%) and 1.89 GPa (85%) for PP/G15 and (PP/GF15)/NC3 composite, respectively. As for the composite with higher clay loading, 139% increment (to 2.44 GPa) in flexural modulus value is observed with the incorporation of 6 and 9 phr NC into the system ((PP/G15)/NC6 and (PP/G15)/NC9). Clay can adhere on the GF surface as well as on the PP matrix, which affects the interfacial properties in the composites such as the adhesive strength and interfacial stiffness of the composite medium.[36,37] These two factors play a crucial role in the stress transfer efficiency and the elastic deformation from the matrix to the reinforcement agents. It is suggested that this could be due to the surface and contact area effect. The high surface area of clay increases the contact area with the matrix, thereby increasing the interface. The enhanced interfacial property and effective stress transfer increases the modulus of the fiber composites based on a nanocomposite matrix.

Conclusions

Layered clays were used as nanoparticle fillers in GF-reinforced PP composites. The concentration of the particles and their distribution in the matrix were observed to be quite important in maximizing the benefits of nanoparticle reinforcement. Exfoliated and

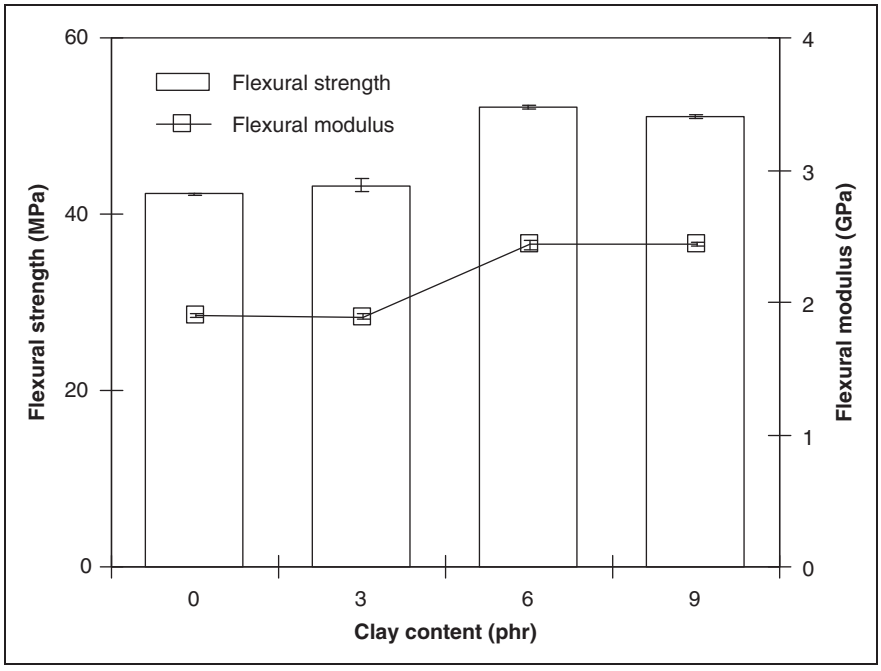

Figure 10. Flexural strength and flexural modulus of 15% W_f GF composite with different clay loadings.

Downloaded from jrp.sagepub.com at HINARI on March 4, 2012

disordered intercalated structures provided the best reinforcement, whereby more ordered intercalated structures offer little benefit. The XRD peaks of the clay nanoparticles in the nanocomposites were shifted to lower intensity by the addition of GF, indicating the fact that clay has partially exfoliated from the stacks of clay layers.

The T_{onset} of PP/GF/NC is seen to have increased by approximately 9°C to 14°C, and simultaneously, the initial thermal stability ($T_{5\%}$ and $T_{10\%}$) is also observed to have increased (up to 56°C and 43°C), respectively, than the conventional PP/GF composite.

Tensile strength and tensile modulus of PP/GF composites decreased and increased, respectively, with an increase in fiber loading. The addition of clay nanoparticles improved these properties. Flexural strength and flexural modulus increased with increase in fiber loading. The addition of clay nanoparticles further improves these properties.

Overall, this study shows that clay nanoparticles can easily be used to modify traditional fiber-reinforced composite materials to enhance their resistance to thermal degradation processes and improve their mechanical properties.

Funding

The work was supported by the University of Malaya [grant number PPP (PS230/2008B, PS376/2009B, and PS504/2010B).

References

1. Chen X, Guo Q and Mi Y. Bamboo fiber-reinforced polypropylene composites: a study of the mechanical properties. *J Appl Polym Sci* 1998; 69(10): 1891–1899.
2. Vilaseca F, Valadez-Gonzalez A, Herrera-Franco PJ, Pèlach M, López JP and Mutjé P. Biocomposites from abaca strands and polypropylene. Part I: Evaluation of the tensile properties. *Bioresour Technol* 2010; 101(1): 387–395.
3. Hong CK, Kim MJ, Oh SH, Lee YS and Nah C. Effects of polypropylene-g-(maleic anhydride/styrene) compatibilizer on mechanical and rheological properties of polypropylene/clay nanocomposites. *J Ind Eng Chem* 2008; 14(2): 236–242.
4. Jordan J, Jacob KI, Tannenbaum R, Sharaf MA and Jasiuk I. Experimental trends in polymer nanocomposites – a review. *Mater Sci Eng A* 2005; 393(1–2): 1–11.
5. Modesti M, Lorenzetti A, Bon D and Besco S. Thermal behaviour of compatibilised polypropylene nanocomposite: effect of processing conditions. *Polym Degrad Stab* 2006; 91(4): 672–680.
6. Samal SK, Nayak SK and Mohanty S. Polypropylene nanocomposites: effect of organo-modified layered silicates on mechanical, thermal & morphological performance. *J Thermoplast Compos Mater* 2008; 21(3): 243–263.
7. Mohan TP and Kanny K. Influence of nanoclay on rheological and mechanical properties of short glass fiber-reinforced polypropylene composites. *J Reinf Plast Compos* 2011; 30(2): 152–160.
8. Chandradass J, Ramesh Kumar M and Velmurugan R. Effect of clay dispersion on mechanical, thermal and vibration properties of glass fiber-reinforced vinyl ester composites. *J Reinf Plast Compos* 2008; 27(15): 1585–1601.
9. ASTM Standard D-638. Standard test method for tensile properties of plastics. West Coshoshocken, PA: ASTM International, 2003, doi: 10.1520/D0638-03, www.astm.org.
10. ASTM Standard D790-10. Standard test methods for flexural properties of unreinforced and reinforced plastics and electrical insulating materials. West Coshoshocken, PA: ASTM International, 2010, doi: 10.1520/D0790-10, www.astm.org.
11. Kanny K, Jawahar P and Moodley VK. Mechanical and tribological behavior of clay–polypropylene nanocomposites. *J Mater Sci* 2008; 43(22): 7230–7238.
12. Lertwimolnun W and Vergnes B. Influence of compatibilizer and processing conditions on the dispersion of nanoclay in a polypropylene matrix. *Polymer* 2005; 46(10): 3462–3471.
13. Haque A, Shamsuzzoha M, Hussain F and Dean D. S2-glass/epoxy polymer nanocomposites: manufacturing, structures, thermal and mechanical properties. *J Compos Mater* 2003; 37(20): 1821–1837.
14. Timmerman JF, Hayes BS and Seferis JC. Nanoclay reinforcement effects on the cryogenic microcracking of carbon fiber/epoxy composites. *Compos Sci Technol* 2002; 62(9): 1249–1258.
15. Ren J, Huang Y, Liu Y and Tang X. Preparation, characterization and properties of poly (vinyl chloride)/compatibilizer/organophilic-montmorillonite nanocomposites by melt intercalation. *Polym Test* 2005; 24(3): 316–323.
16. Bozkurt E, Kaya E and Tanoglu M. Mechanical and thermal behavior of non-crimp glass fiber reinforced layered clay/epoxy nanocomposites. *Compos Sci Technol* 2007; 67(15–16): 3394–3403.
17. Hussain F, Roy S, Narasimhan K, Vengadassalam K and Lu H. E-Glass–polypropylene pultruded nanocomposite: manufacture, characterization, thermal and mechanical properties. *J Thermoplast Compos Mater* 2007; 20(4): 411–434.
18. Hwang TY, Lee SM, Ahn Y and Lee JW. Development of polypropylene-clay nanocomposite with supercritical CO_2 assisted twin screw extrusion. *Korea-Aust. Rheol J* 2008; 20(4): 235–243.
19. Krump H, Luyt AS and Hudec I. Effect of different modified clays on the thermal and physical properties of polypropylene-montmorillonite nanocomposites. *Mater Lett* 2006; 60(23): 2877–2880.
20. Duquesne S, Jama C, Le Bras M, Delobel R, Recourt P and Gloaguen JM. Elaboration of EVA-nanoclay systems – characterization, thermal behaviour and fire performance. *Compos Sci Technol* 2003; 63(8): 1141–1148.
21. Sharma SK and Nayak SK. Surface modified clay/polypropylene (PP) nanocomposites: effect on

Downloaded from jrp.sagepub.com at HINARI on March 4, 2012

physico-mechanical, thermal and morphological properties. *Polym Degrad Stab* 2009; 94(1): 132–138.
22. Oksman K, Mathew AP, Långström R, Nyström B and Joseph K. The influence of fibre microstructure on fibre breakage and mechanical properties of natural fibre reinforced polypropylene. *Compos Sci Technol* 2009; 69(11–12): 1847–1853.
23. Thomason JL. The influence of fibre length and concentration on the properties of glass fibre reinforced polypropylene: 5. Injection moulded long and short fibre PP. *Compos Part A* 2002; 33(12): 1641–1652.
24. Mohd Ishak ZA, Ariffin A and Senawi R. Effects of hygrothermal aging and a silane coupling agent on the tensile properties of injection molded short glass fiber reinforced poly (butylene terephthalate) composites. *Eur Polym J* 2001; 37(8): 1635–1647.
25. Hussain M, Nakahira A and Niihara K. Mechanical property improvement of carbon fiber reinforced epoxy composites by Al2O3 filler dispersion. *Mater Lett* 1996; 26(3): 185–191.
26. Zhao R, Huang J, Sun B and Dai G. Study of the mechanical properties of mica-filled polypropylene-based GMT composite. *J Appl Polym Sci* 2001; 82(11): 2719–2728.
27. Lee NJ and Jang J. The effect of fibre content on the mechanical properties of glass fibre mat/polypropylene composites. *Compos Part A* 1999; 30(6): 815–822.
28. Hiscock DF and Bigg DM. Long fiber reinforced thermoplastic matrix composites by slurry deposition. *Polym Compos* 1989; 10(3): 145–149.
29. Fu SY and Lauke B. Characterization of tensile behaviour of hybrid short glass fibre/calcite particle/ABS composites. *Compos Part A* 1998; 29(5–6): 575–583.
30. Thomason JL, Vlug MA, Schipper G and Krikor H. Influence of fibre length and concentration on the properties of glass fibre-reinforced polypropylene: Part 3. Strength and strain at failure. *Compos Part A* 1996; 27(11): 1075–1084.
31. Hassan A, Normasmira AR and Yahya R. Extrusion and injection-molding of glass fiber/MAPP/polypropylene: effect of coupling agent on DSC, DMA and mechanical properties. *J Reinf Plast Compos* 2011; 30(14): 1223–1232.
32. Hussain M, Oku Y, Nakahira A and Niihara K. Effects of wet ball-milling on particle dispersion and mechanical properties of particulate epoxy composites. *Mater Lett* 1996; 26(3): 177–184.
33. Wetzel B, Haupert F and Qiu Zhang M. Epoxy nanocomposites with high mechanical and tribological performance. *Compos Sci Technol* 2003; 63(14): 2055–2067.
34. Asi O. Mechanical properties of glass-fiber reinforced epoxy composites filled with Al_2O_3 particles. *J Reinf Plast Compos* 2009; 28(23): 2861–2867.
35. Kornmann X, Rees M, Thomann Y, Necola A, Barbezat M and Thomann R. Epoxy-layered silicate nanocomposites as matrix in glass fibre-reinforced composites. *Compos Sci Technol* 2005; 65(14): 2259–2268.
36. Wetzel B, Haupert F, Friedrich K, Zhang MQ and Rong MZ. Impact and wear resistance of polymer nanocomposites at low filler content. *Polym Eng Sci* 2002; 42(9): 1919–1927.
37. Norkhairunnisa M, Azhar AB and Shyang CW. Effects of organo montmorillonite on the mechanical and morphological properties of epoxy/glass fiber composites. *Polym Int* 2007; 56(4): 512–517.

Downloaded from jrp.sagepub.com at HINARI on March 4, 2012